HHS Public Access

Author manuscript

Eur Neuropsychopharmacol. Author manuscript; available in PMC 2016 August 01.

Published in final edited form as:

Eur Neuropsychopharmacol. 2015 August ; 25(8): 1342–1352. doi:10.1016/j.euroneuro.2015.04.008.

Altered voltage-gated calcium channels in rat inferior colliculus neurons contribute to alcohol withdrawal seizures

Prosper N'Gouemo

Department of Pediatrics, Georgetown, University Medical Center, Washington, DC, USA

Abstract

We have previously reported that enhanced susceptibility to alcohol withdrawal seizures (AWS) parallels the enhancement of the current density of high-threshold voltage-gated Ca^{2+} (Ca_V) channels in rat inferior colliculus (IC) neurons. However, whether this increased current density is a cause or consequence of AWS is unclear. Here, I report changes in the current density of Ca_V channels in IC neurons during the course of alcohol withdrawal and the potential anticonvulsant effect of intra-IC infusions of L- and P-type Ca_V channel antagonists. Whole-cell currents were activated by depolarizing pulses using barium as the charge carrier. Currents and seizure susceptibility were evaluated in control animals 3 h after alcohol intoxication, as well as 3 h (before AWS), 24 h (when AWS susceptibility is maximal), and 48 h (when AWS susceptibility is no longer present) after alcohol withdrawal. Nifedipine, nimodipine (L-type antagonists) or ω-agatoxin TK (P-type antagonist) were infused intra-IC to probe the role of Ca_V channels in the pathogenesis of AWS. Ca_V current density and conductance in IC neurons were significantly increased 3 and 24 h after alcohol withdrawal compared with the control group or the group tested 3 h following ethanol intoxication. Blockade of L-type Ca_V channels within the IC completely suppressed AWS, and inhibition of P-type channels reduced AWS severity. These findings suggest that the enhancement of Ca_V currents in IC neurons occurs prior to AWS onset and that alterations in L- and P-type Ca_V channels in these neurons may underlie the pathogenesis of AWS.

Keywords

ω-agatoxin TK; nifedipine; nimodipine; calcium channels; current density; generalized tonic-clonic seizures

1. Introduction

Neuronal hyperexcitability following the cessation of chronic alcohol intake (alcohol withdrawal) often leads to enhanced susceptibility to generalized tonic-clonic seizures

Address correspondence to: Prosper N'Gouemo, Georgetown University Medical Center, Department of Pediatrics, Building D, Room 285, 3900 Reservoir Rd, NW, Washington, DC 20057, Tel: (202) 687-8464; Fax: (202) 687-6914, pn@georgetown.edu.

Conflict of interest

None.

(GTCS). The inferior colliculus (IC) is critical for the initiation of acoustically evoked reflex GTCS (audiogenic seizures, AGS) in rats subjected to alcohol withdrawal (Chakravarty and Faingold, 1998; Faingold and Riaz, 1995; Eckardt et al., 1986; Frye et al., 1983; McCown and Breese, 1990, 1993; Riaz and Faingold, 1994). Electrophysiological studies report increased IC neuronal firing prior to and during AGS in animals subjected to alcohol withdrawal (Chakravarty and Faingold, 1998). Similarly, in vitro studies show elevated IC neuronal excitability during alcohol withdrawal (Evans et al., 2000). These functional findings confirm the importance of IC neurons in networks involved in alcohol withdrawal seizures (AWS, Faingold et al., 1998). Voltage-gated Ca^{2+} (Ca_V) channels play an important role in the neuronal hyperexcitability that leads to AGS during alcohol withdrawal, as indicated by the suppression of these seizures by L-type channel blockade (Little et al., 1986). Furthermore, we have reported an enhancement of the current density of L- and P-type high-threshold Ca_V channels in IC neurons 24 h during alcohol withdrawal, when the susceptibility to AGS is peaked (N'Gouemo and Morad, 2003). At 48 h, when the susceptibility to AWS was no longer present, Ca_V channel currents returned to nearly control levels (N'Gouemo and Morad, 2003). Recently, a time-course study reported that AGS susceptibility was absent in the first 7 h but progressively develops after 7 h, peaking at 24 h and disappearing at 48 h during alcohol withdrawal (Faingold, 2008). It is unknown whether the enhanced Ca_V channel currents found in IC neurons precedes the onset of AWS susceptibility. The roles of L- and P-type Ca_V channels within the IC in the pathogenesis of AWS are also unknown. Here, I report the possible role of enhancement of Ca_V channel currents in IC neurons in the pathogenesis of AWS.

2. Experimental procedures

2.1. Animals

Male Sprague-Dawley (250–300 g, Taconic, Germantown, MD, USA) rats were used. Animals were maintained in a temperature/humidity-controlled room on a 12 h/12 h light/dark cycle with free access to food and water. All possible efforts were made to minimize the number of animals used in experiments. All experimental procedures were approved by the Georgetown University Animal Care and Use Committee and followed the NIH Guide for the Care and Use of Laboratory Animals.

2.2. Cannula guide implantation

Animals were anesthetized with ketamine/xylazine (85/3 mg/kg i.p.). Guide cannulae (21-gauge, Plastics One, Roanoke, VA, USA) were implanted bilaterally over the IC (−9.15 mm posterior to bregma, ±1.5 mm lateral to bregma), and the injection cannula was subsequently inserted vertically to 4.5 mm below the surface of the brain (Paxinos and Watson 1998). A stylet was placed in each guide cannula to prevent clogging when not in use.

2.3. Ethanol administration

Five to seven days after stereotaxic surgery, animals were subjected to chronic ethanol intoxication. Ethanol (95%) was administered by intragastric intubation in rats in a 30% v/v solution in ISOMIL Infant Formula. Ethanol administration consisted of three doses every 8 h for 4 days, and the levels of intoxication was evaluated using a standard behavior rating

scale (Majchrowicz, 1975; Faingold, 2008). The priming dose of ethanol was 5 g/kg (body weight), and the subsequent doses were adjusted for each animal to maintain a moderate degree of ataxia. The daily amount of ethanol administered varied from 9 to 15 g/kg (body weight) for each animal; these amounts allowed intoxication to be maintained at a level sufficient to achieve a consistent, moderate ataxia. Ethanol administration was ceased on the fourth day, after the second daily dose. The behavioral signs of ethanol withdrawal consisted of hyperactivity, tremors, tail spasticity, and spontaneous seizures (myoclonus, forelimb clonic seizures), and ethanol withdrawal induced episodes of acoustically evoked startle and seizures. To determine the effects of ethanol intoxication, animals received a single dose of ethanol (5 mg/kg body weight, p.o.). Control animals were maintained under similar conditions and schedules but were fed only the ISOMIL without ethanol. Weight loss and the incidence of mortality were negligible. Animals used for electrophysiological studies were not subjected to acoustically evoked seizure testing because long-lasting increases in extracellular GABA levels have been observed as a result of evoked seizures (Ueda and Tsuru, 1995). Such released GABA and various degree seizure severity and duration may alter Ca_V channel currents.

2.4. Seizure testing

To analyze seizure susceptibility of various groups, two animals from each group were randomly selected and tested for AGS at 2–4 h (3 h group), 22–24 h (24 h group) and 46–48 h (48 h group) during ethanol withdrawal, as well as at 2–4 h (3 h group) during ethanol intoxication. The acoustic stimuli (pure tones or mixed sounds at 100–110 decibel sound pressure levels; Med Associated, St. Alban, VT) were presented until either wild running seizures (WRS) were elicited or 60 s passed with no seizure activity. Convulsive seizure behavior was classified into four stages: stage 0, no seizures in response to acoustic stimuli; stage 1, one episode of WRS and/or jumping; stage 2, two episodes of WRS and/or jumping; stage 3, one episode of WRS and/or jumping followed by bouncing GTCS (clonus). WRS and clonus correspond to the pre-convulsive and convulsive phases of AGS, respectively.

2.5. Focal microinjection

For microinjection procedures, stylets were removed from the implanted cannula guide tubes, and vehicle (phosphate buffer, pH 7.4) was infused through an injection cannula (26 gauge, Plastics One) at a rate of 0.25 μL/min for 2 min (Millan et al 1986). Animals were then tested for susceptibility to AGS. Only animals exhibiting AGS during ethanol withdrawal were used for focal pharmacological studies. Animals were closely monitored following administration of ω-agatoxin TK (30 nM/side), nifedipine (10 μM/side) or nimodipine (1 μM/side). Animals were tested for AGS susceptibility at 0.5, 1 and 2 h post infusion. In another set of control experiments, animals that exhibited AGS after microinjection of the vehicle were tested at 0.5, 1 and 2 h. At the end of the experiment, the animals received bilateral infusions of Fast green (0.5 μL/side, Electron Microscopy Science, Hatfield, PA, USA) at the microinjection sites. Animals were then deeply anesthetized with Nembutal (100 mg/kg i.p.), and coronal sections of the IC were obtained to microscopically verify the sites of microinjections.

2.6. Blood ethanol levels

In another set of experiments, blood ethanol concentrations (BECs) were measured in the control group, at 3 h following administration of a single dose of ethanol (5 mg/kg, body weight, ethanol intoxication group) as well as at 3, 24 and 48 h during ethanol withdrawal. Blood samples were collected in anesthetized animals (Nembutal 50 mg/kg i.p.) by intracardiac sampling using 21-gauge needles. Serum ethanol concentrations were measured using an Analox model GM7 Micro Stat analyzer (Analox Instruments, London, UK).

2.7. Cell preparation

Controls and rats subjected to ethanol intoxication and withdrawal were anesthetized with Nembutal (50 mg/kg, body weight, i.p.). The brains were perfused with a solution containing (in mM) 110 choline chloride, 2.5 KCl, 1.2 NaH_2PO_4, 26 $NaHCO_3$, 2.4 sodium/pyruvate, 1.3 L-ascorbic acid, 20 mM dextrose, 0.5 $CaCl_2$ and 7 $MgCl_2$ (adjusted to 290–300 mOsm with sucrose, bubbled with 95% O_2 and 5% CO_2). Brains were removed and coronal IC slices (400 μM thick) were sectioned using a Leica VT1200S Vibratome (Leica Microsystems Inc., Buffalo Grove, IL, USA). The cutting solution contained (in mM) 205 sucrose, 5 KCl, 1.2 NaH_2PO_4, mM $NaHCO_3$, 2.4 sodium/pyruvate, 1.3 L-ascorbic acid, 20 dextrose, 0.2 $CaCl_2$, and 1.3 $MgSO_4$ (adjusted to 290–300 mOsm with sucrose, bubbled with 95% O_2 and 5% CO_2). The central nucleus of the IC was dissected and placed in Leibovitz's L-15 medium (Life Technologies, Gaithersburg, MD, USA) containing papain (20 U/mL; Worthington, Lakewood, NJ, USA) for 60 min (at 30–32°C and bubbled with 100% oxygen). The enzyme was washed with Leibovitz's L-15 medium containing ovomucoid inhibitor-albumin (1 mg/mL; Worthington). Neurons were then dissociated by gentle trituration with a fire-polished Pasteur pipette in Neurobasal-A medium (Life Technologies) supplemented with 2% B27 (Life Technologies), penicillin (100 U/mL) and streptomycin (0.1 mg/mL). The dissociated IC neurons were then plated onto concanavalin-A (100 mg/mL)-coated glass coverslips and placed in a CO_2 incubator at least 1 h prior to the start of voltage clamp experiments.

2.8. Electrophysiology

Ca^{2+} channel currents were recorded at room temperature using whole-cell patch clamp techniques (Hamill et al., 1981). The patch electrodes were made from borosilicate glass capillary tubes and had 3 to 4 ΩM resistances when filled with a solution containing (in mM) 90 cesium methanesulfonate, 10 EGTA, 30 phosphocreatine, 10 HEPES, 10 glucose, 4 Na_2-ATP, 5 $MgCl_2$ and 0.4 Na-GTP (adjusted to pH 7.3 with CsOH). A whole-cell recording configuration was established in a solution containing (in mM) 145 NaCl, 5.4 KCl, 2 $CaCl_2$, 1 $MgCl_2$, and 10 HEPES (adjusted to pH 7.4 with NaOH). The extracellular recording solution for isolating barium (Ba^{2+}) currents contained (in mM) 5 $BaCl_2$, 130 TEACl, 10 HEPES, 1 $MgCl_2$, 20 $CsCl_2$, 10 glucose and 0.001 TTX (adjusted to pH 7.4 with TEAOH). Although Ca^{2+} is the biological charge carrier through Ca^{2+} channels, Ba^{2+} was instead selected to be used to characterize Ca^{2+} currents. Ba^{2+} permeates Ca^{2+} channels as well as Ca^{2+} but does not inactivate the channels. In addition, Ba^{2+} suppresses residual K^+ currents. Thus, Ba^{2+} currents were referred to as Ca_V channel currents. Voltage clamp experiments were performed with either a Dagan 8900 (Dagan Corporation, Minneapolis,

MN, USA) or MultiClamp B patch clamp amplifier (Molecular Devices, Sunnyvale, CA, USA). Currents were filtered at 10 kHz and normalized relative to the membrane capacitance as an estimate of current density. Whole cell capacitance and series resistance were compensated, and leak and residual capacitance currents were subtracted. Whole cell measurements were corrected for liquid junction potentials and currents were recorded from relatively large IC neurons (~22 μm in diameter).

Voltage protocols—IC neurons were held at −80 mV unless otherwise stated. A 0.5-s conditioning pulse to −60 mV was first applied to inactivate low-threshold voltage-activated Ca^{2+} channels. Ba^{2+} currents were then activated by applying voltage steps to 0 mV at 10-s intervals until a stable recording was obtained. The voltage step to 0 mV was chosen because the resulting peak current density was maximal compared with other tested voltage steps in IC neurons (N'Gouemo and Morad, 2003). Peak Ba^{2+} currents were measured 5-ms after the start of the test pulse, in part to approximate the action potential duration (which is ~1-ms at half-maximal amplitude, Li et al., 1994). To determine current-voltage relationships, currents were evoked by using 50-ms depolarizing pulses from a holding potential of −90 mV (depolarization range: −90 mV to +60 mV by 10 mV increments).

2.9. Statistical analysis

Statistical analyses were performed using OriginPro 9.1 software (Origin, Northampton, MA, USA) and Primer Biostatistics program version 6.0 software (The McGraw Hill Education, New York, NY, USA). Data were collected using Clampex v10 and analyzed off-line using Clampfit v10 (Molecular Devices) and Origin 9.1 software (Origin). The voltage dependence of peak Ba^{2+} current density was fitted using the following modified Boltzmann equation: $I=[G_{max} \times (V-V_{rev})]/[1+\exp\{(V_{0.5}-V)/k\}]$, where I (V) is the peak current density at the command potential V, G_{max} is the maximum conductance, V_{rev} is the reversal potential, $V_{0.5}$ is the half-activation potential, and *k* is the slope factor. The conductance ($G=I/V-V_{rev}$) was determined at each command potential (V). The voltage dependence of Ba^{2+} conductance was plotted as a function of the test pulse and was best fit with a modified Boltzmann equation: $G=G_{max}/[1+\exp^{(-(V-V_{0.5})/k)}]$, where G_{max} is the maximum conductance, generating values for conductance (G) at the potential $V_{0.5}$ and the slope factor *k*. The modified Boltzmann equation was also used to calculate G_{max} in the control group, during ethanol intoxication and ethanol withdrawal. To determine differences in Ba^{2+} current density and conductance, one-way analyses of variance (ANOVA) with Bonferroni tests for *post hoc* comparisons were performed. Data were first subjected to a normality test (Kolmogorov-Smirnov) and tests for homogeneity of variance (Levene's test and Brown-Forsythe's test) before ANOVA. For in vivo pharmacological studies and seizure testing, animals that did not display seizures within the 60-sec acoustic stimulation period were considered to be protected from seizure activity. For each group, the incidences of WRS and clonus were recorded and analyzed using the McNemars test (χ^2). The seizure severity score was analyzed using the Kruskal-Wallis test. A value of $P<0.05$ was considered statistically significant. Data on BECs, current densities, and conductance are presented as the mean±S.E.M., or median seizure score±S.E.M. for seizure severity and the percentage (%) for the incidence of WRS and clonus. Current trace illustrations represent the average of 3–5 consecutive traces.

3. Results

3.1. Seizure susceptibility during ethanol intoxication and withdrawal

Figure 1 (panel 1A) demonstrates AGS susceptibility in the control group, at 3 h during ethanol intoxication, and at several time points (3, 24 and 48 h) during ethanol withdrawal period. AGS in rats subjected to ethanol withdrawal consisted of WRS followed by clonus. This seizure phenotype was observed in all animals tested 24 h after ethanol withdrawal (n=10). The seizure susceptibility was transient and occurred during a finite period. Specifically, no seizures were observed at 3 h (n=8) or 48 h (n=8) after the initiation of the ethanol withdrawal period or at 3 h during ethanol intoxication (n=8); nor were any seizures observed in the control group (n=8) at those time points.

3.2. Blood ethanol concentrations during ethanol intoxication and withdrawal

Figure 1 (panel B) reveals that BECs were significantly elevated 3 h during ethanol intoxication (0.38±0.05 g/dL, n=6) compared with the control group (0.007±0.001 g/dL, n=6, t=9, $P<0.05$) and 3 h during ethanol withdrawal (0.25±0.04 g/dL, n=6, t=3, $P<0.05$). During ethanol withdrawal, BECs were also significantly elevated at 3 h (0.25±0.04 g/dL, n=6, t=6, $P<0.05$) but negligible at 24 h (0.010±0.001 g/dL, n=6) and 48 h (0.011±0.001 g/dL, n=6) compared with the control group (0.007±0.001 g/dL, n=6). BECs of the 3 h group during ethanol withdrawal also were significantly elevated compared to 24 h (t=6, $P<0.5$) and 48 h (t=6, $P<0.05$) group.

3.3. Altered Ca^{2+} channel currents during ethanol intoxication and withdrawal

Figure 1 (panel 1C) shows the mean of the peak Ba^{2+} currents in IC neurons obtained from the control group 3 h after ethanol intoxication and at 3, 24 and 48 h during ethanol withdrawal. ANOVA revealed that group means were significantly different (F= 19, $P<0.001$). Interestingly, the peak Ba^{2+} current density evoked at 0 mV was significantly enhanced both before the onset of AWS susceptibility (3 h; 27±1 pA/pF, n=14, t=5, $P<0.05$) and when the incidence of AWS was highest (24 h; 31±1 pA/pF, n=18, t=8, $P<0.05$) during ethanol withdrawal compared with the control group (20±1 pA/pF, n=16). At 48 h during ethanol withdrawal, when seizure susceptibility was no longer present, the current density (24±1 pA/pF, t=3, $P<0.05$, n=16) remained significantly elevated compared to the control group (20±1 pA/pF, n=16). The mean of the peak current density at 24 h (31±1 pA/pF, n=18, t=5, $P<0.05$) but not at 3 h during ethanol withdrawal was also significantly enhanced compared with 48 h (24±1 pA/pF, n=16) during ethanol withdrawal. The peak current density was only slightly increased at 24 h (31±1 pA/pF, n=18) compared to 3 h (27±1 pA/pF, n=14) during ethanol withdrawal. Quantification of the data also showed that ethanol withdrawal enhanced the current density compared with ethanol intoxication. Notably, the current density at 3 h following ethanol withdrawal (27±1 pA/pF, n=14, t=3, $P<0.05$) was significantly elevated compared with 3 h following ethanol intoxication (21±2 pA/pF, n=10). Ethanol intoxication (21±2 pA/pF, n=10) did not alter the current density in IC neurons compared with the control group (20±1 pA/pF, n=16). The increase in Ca^{2+} currents was not accompanied by a significant change in cell capacitance (control group: 71±4 pF, n=16; 3 h ethanol intoxication: 71±5 pF, n=10; ethanol withdrawal: (i) 3 h group: 72±5 pF, n=14; (ii) 24 h group: 73±5 pF, n=18; and (iii) 48 h: 73±5 pF, n=16).

Figure 2 shows the original traces of total Ba^{2+} currents evoked at a range of voltages from five representative IC neurons obtained from the control group (panel 2A), 3 h after ethanol intoxication (panel 2B) or 3 h (panel 2C), 24 h (panel 2D) or 48 h (panel 2E) following ethanol withdrawal. The voltage protocol is showed in panel 2E. At the voltage command of −20 mV, the current density was enhanced 2.3-fold at 24 h following ethanol withdrawal compared with the control group, the group tested 3 h following ethanol withdrawal and the group tested 3 h after ethanol intoxication. Similarly, ethanol withdrawal enhanced the current density 2-fold at 48 h compared with the control group, the group tested 3 h following ethanol withdrawal or the group tested 3 h after ethanol intoxication.

3.4. Ethanol withdrawal alters the voltage-dependence of Ca^{2+} channel currents

Quantification of the currents over a larger range of voltages (−90 mV to +60 mV, Figure 3) revealed that the activation of peak Ba^{2+} currents occurred at −34±2 mV in four conditions: in the control group (n=14; panels 3A,B; filled squares), at 3 h during ethanol intoxication (n=7; panel 3A; filled diamonds), and at 3 h (n=10; panels 3A,B; filled triangles) and 48 h (n=10; panels 3A,B; filled octagons) during ethanol withdrawal. At 24 h during ethanol withdrawal, however, activation of peak Ba^{2+} currents occurred at −53±3 mV (n=11; panels 3A,B), which was significantly lower than in the other four groups (t=7, P<0.0, panel B; filled circles). Figure 3A evaluates the current density in the control group, 3 h during ethanol intoxication and 3 h during ethanol withdrawal. Comparison of the current-voltage relationship between the control group (filled squares, panel 3A) and the group tested 3 h during ethanol intoxication (filled diamonds, panel 3A) showed a +10 mV shift in the maximal value of the peak current and no change in the magnitude of the peak current density at voltages between −90 mV and +60 mV. Comparison of the current-voltage relationship between the control group (filled squares) and the group tested 3 h during ethanol withdrawal (filled triangles, panels 3A,B) showed a significant (P<0.05) increase in the current density by an average of 47% at voltages between −10 mV and +40 mV (panels 3A,B). This enhancement of the current density was accompanied by a +10 mV shift in the test potential 3 h during ethanol withdrawal (panels 3A,B). Similarly, the current density at 3 h during ethanol withdrawal (filled triangles, panel A) was also significantly (t=4, P<0.05) elevated at 0 mV compared to 3 h during ethanol intoxication (filled diamonds, panel A). Figure 3B evaluates changes in the current density during ethanol withdrawal. Quantification of the data showed that the peak Ba^{2+} current density at 24 h during ethanol withdrawal (filled circles, panel 3B) exhibited, on average, a 3-fold increase (P<0.05) at voltages between −40 mV and 0 mV compared with 3 h during ethanol withdrawal (filled triangles, panel B). This enhancement of the currents was associated with −15 mV shifts in the maximum of the peak Ba^{2+} currents. When compared with the control group (filled squares), the group assayed 24 h during ethanol withdrawal (filled circles) exhibited, on average, 1.3-fold increases (P<0.05) in the current density over a large range of voltages between −40 mV and +40 mV. Figure 3B also shows that the peak current density at 24 h during ethanol withdrawal (filled circles) was significantly elevated by a mean of 3.5-fold at voltages between −40 mV and 0 mV compared with the group assayed 48 h during ethanol withdrawal (filled octagons). Quantification of these data also showed that the current density in IC neurons remained non-significantly increased by 28% at voltages between −20

mV and +50 mV at 48 h during ethanol withdrawal (filled octagons) compared with the control group (filled squares).

3.5. Ethanol withdrawal alters Ca^{2+} channel conductance and voltage-dependence

Figure 4 (panels 4A,C,D) shows the Ba^{2+} conductance and voltage relationships in the control group (filled squares), in the group tested 3 h after ethanol intoxication (filled diamonds) and in the group tested 3 h during ethanol withdrawal. Figure 4 (panels B,C,E) also shows the Ba^{2+} conductance and voltage relationships in the control group (filled squares) and in groups tested at several time points, including at 3 (filled triangles), 24 (filled circles) and 48 h (filled octagons) during ethanol withdrawal. The most prominent changes include the following: i) 34% and 31% increases in conductance compared with the control group at voltages above 0 mV at 3 h and 24 h during ethanol withdrawal, respectively (panel 4B) and ii) significantly ($F=4$, $P<0.01$, panel 4C) elevated mean G_{max} values of 47% and 44% at 3 h (0.47±0.03 pS/pF, n=10, $t=3$, $P<0.05$) and 24 h (0.46±0.04 pS/pF, n=11, $t=3$, $P<0.05$) following ethanol withdrawal, respectively, compared to the control group (0.32±0.02 pS/pF, n=14). G_{max} values were not significantly increased 3 h after ethanol intoxication (0.4±0.03 pS/pF, n=7, panel 4C) compared with the control group (0.32±0.02 pS/pF, n=14) and the group tested 3 h following ethanol withdrawal (0.47±0.03 pS/pF, n=10). No significant changes in G_{max} values were found at 48 h (0.38±0.05 pS/pF, n=10) following ethanol withdrawal compared with the control group (0.32±0.02 pS/pF, n=14, panel 4C). G/G_{max} curves (Fig. 4, panel D) revealed that the activation parameter $V_{0.5}$ non-significantly shifted toward more positive values at 3 h after ethanol intoxication (−15±2 mV, n=7) and at 3 h (−14±2 mV, n=10) during ethanol withdrawal compared with the control group (−19±2 mV, n=14). G/G_{max} curves (Fig. 4, panel E) also revealed that the activation parameter $V_{0.5}$ non-significantly shifted toward more positive values at at 3 h (−14±2 mV, n=10) and 48 h (−15±1 mV, n=10) during ethanol withdrawal but shifted toward a negative value at 24 h (−30±3 mV, n=11) during ethanol withdrawal compared with the control group (−19±2 mV, n=14). Nevertheless, the activation parameter $V_{0.5}$ was significantly shifted toward negative values at 24 h during ethanol withdrawal (−30±3 mV, n=11) compared with the groups tested 3 h (−14±2 mV, n=10; $t=-5$, $P<0.05$) and 48 h (−15±1 mV, n=10; $t=5$, $P<0.05$) after ethanol withdrawal as well as the control group (−19±2 mV, n=14, $t=-4$, $P<0.05$). Ethanol withdrawal did not alter the mean value of the slope factor of activation (*k)* at 3 h (4.7±0.4, n=10), 24 h (2.6±0.3, n=11) or 48 h (3.1±0.1, n=10) during ethanol withdrawal compared with the control group (3.2±0.2, n=14). Ethanol intoxication also did not modify the mean value of the slope factor of activation (4±0.4, n=7) compared with the control group (3.2±0.4, n=14) or the group tested 3 h durining ethanol withdrawal (4.7±0.4, n=10).

3.6. Focal administration of Ca^{2+} channel blockers within the inferior colliculus suppresses alcohol withdrawal seizures

Figure 5 reveals the anticonvulsant potential of potent blockers of L- (nifedipine and nimodipine) or P-type (ω-agatoxin TK) Ca_V channels. Panels 5A and B, 5C and D, and 5E and 5F show the effects of bilateral microinjections of ω-agatoxin TK (30 nM/side), nifedipine (10 μM/side) and nimodipine (1 μM/side), respectively, on the time course of seizure severity (median score) and on the incidence of WRS and clonus following ethanol

withdrawal. Kruskal-Wallis ANOVA showed that bilateral microinjections of ω-agatoxin TK did not significantly (Kruskal-Wallis=2, P<0.1, panel A) alter seizure severity during the first 2 h following treatment. Focal microinjections of either nifedipine (Kruskal-Wallis=11, P<0.01, panel C) or nimodipine (Kruskal-Wallis=12, P<0.01, panel E) significantly reduced seizure severity during the first 2 h following treatment. The time course also revealed that the most potent effects of ω-agatoxin TK, nifedipine and nimodipine were observed at 2 h post infusion within the IC (panels A,C,E). Thus, bilateral intra-IC microinjections of ω-agatoxin TK (panel A) and nifedipine (panel C) reduced the median seizure severity from 3 to 1 (n=6) and from 3 to 0.5 (n=6), respectively, while infusions of nimodipine (panel E) produced a complete suppression of the seizures (from a median seizure severity of 3 to 0, n=6). Note that at 30 min post infusion within the IC, ω-agatoxin TK and nifedipine reduced the seizure severity score from 3 to 2.5 (n=6, panel A) and from 3 to 2 (n=6, panel C), respectively, while nimodipine markedly reduced the seizure severity score from 3 to 0.5 (n=6, panel E). Quantification at 2 h post infusion showed that ω-agatoxin TK (panel 5B), nifedipine (5D) and nimodipine (5F) significantly (P<0.001) reduced the incidence of WRS by 33% (χ^2=67, P<0.001), 50% (χ^2=48, P<0.001) and 83% (χ^2=15, P<0.001), respectively, compared with pre-drug conditions. The incidence of clonus was significantly reduced by 67% (χ^2=31, P<0.001) and 83% (χ^2=15, P<0.001) after microinjections of agatoxin TK and nifedipine but was completely suppressed (χ^2=98, P<0.001) after nimodipine infusion into the IC. Microinjections of the vehicle into the IC did not affect the incidence or severity of acoustically evoked AGS following ethanol withdrawal. Notably, a median seizure severity score of 3 was found at 0.5, 1, and 2 h after bilateral microinjection of the vehicle into the IC. Histological analysis showed that the microinjection sites were within the central nuclei of the IC.

4. Discussion

The major findings of this report are that *i*) the current density of high-threshold Ca_V channels in IC neurons was significantly enhanced before the onset of susceptibility to AWS and *ii*) focal administration of L-type and to a lesser extent of P-type Ca_V channel blockers within the IC markedly reduced the occurrence of GTCS during alcohol withdrawal. The finding that the increase in Ca_V current density occurs prior to the onset of AWS susceptibility, but not following alcohol intoxication, suggests that these changes are not induced by seizure activity but may instead represent an important factor in the etiology of alcohol withdrawal hyperexcitability that leads to seizures. The lack of AWS susceptibility at 3 h during alcohol withdrawal may be due to elevated BECs.

The precise mechanisms underlying the upregulation of high-threshold Ca_V channel currents in IC neurons prior to the onset of AWS remain unknown. In this study, significant increases were found in the mean value of G_{max} at 3 h and 24 h following alcohol withdrawal but not at 3 h after alcohol intoxication. However, these changes in G_{max} values were not accompanied by significant changes in the channel activation $V_{0.5}$ compared with controls, suggesting that alcohol withdrawal does not significantly alter the gating and permeation properties of Ca_V channels before the onset of AWS. Thus, enhancement of Ca_V channel currents in IC neurons at 3 h following alcohol withdrawal may be due to an upregulation of the surface expression of the channels. Interestingly, it has been suggested that the increased

Ca_V channel currents in hippocampal neurons obtained from ethanol-tolerant mice during the withdrawal period may be due to an increase in the number of functioning Ca_V channels, as no changes in their gating and permeability were found (Huang and McArdle, 1993).

The IC neurons play an important role in AGS initiation following alcohol withdrawal (Faingold et al., 1998, for review). Pharmacological studies report that systemic administration of L-type Ca_V channels suppresses AGS during alcohol withdrawal, suggesting that remodeling of these channels occurs, at least in IC neurons, and contributes to the pathogenesis of AWS (Little et al., 1986). Consistent with this hypothesis, we have previously reported an enhancement of L- and P-type Ca_V channel currents in IC neurons during alcohol withdrawal when the susceptibility to seizures was maximal (N'Gouemo and Morad, 2003). These findings suggest a possible causal relationship between the upregulation of L- and P-type Ca_V channels in IC neurons and the occurrence of AWS. L- and P-type CaV channels play important roles in synaptic plasticity and glutamate release, respectively (Thiagarjan et al 2005; Ermolyuk et al 2013). The enhancement of L-and P-type Ca_V currents in IC neurons during alcohol withdrawal is likely to prolong somatic action potentials, increasing the likelihood of bursting behaviors and enhanced neurotransmitter release, thus providing for increased AWS susceptibility. The present study demonstrates that inhibition of L-type Ca_V channels markedly reduces the severity of AWS. Thus, the enhancement of Ca_V channel currents observed in IC neurons prior to the onset of AWS is likely not a consequence of seizure activity. The phenotypes of Ca_V channels that contribute to the observed elevated current density were not pharmacologically identified in this study. Nevertheless, we have previously reported that enhancement of the currents in IC neurons is specifically limited to L- and P-type high-threshold Ca_V channels when the susceptibility to AWS is peaked (N'Gouemo and Morad, 2003). It is possible that these Ca_V channel currents are also enhanced before the onset of AWS. Notably, our recent data demonstrate that the expression of mRNA associated with $Ca_V1.3$ but not $Ca_V1.2$ L-type channels is upregulated in IC neurons before the onset of AWS susceptibility (N'Gouemo et al., 2015). This upregulation may therefore represent a molecular mechanism for the enhancement of the currents before the onset of AWS.

Ca_V channels and Ca^{2+}-dependent mechanisms are thought play an important role in the neuronal hyperexcitability that leads to seizures because intracellular Ca^{2+} levels rise and extracellular Ca^{2+} levels decrease during seizure activity (Heinemann et al., 1977). The enhancement of Ca_V channel currents has also been suggested as a possible mechanism for the generation of AWS, as the activation of L-type Ca_V channels has been shown to increase alcohol withdrawal hyperexcitability, while the blockade of these channels has the opposite effect (Whittington and Little, 1993; Whittington et al., 1993; present study). The mechanisms by which elevated Ca_V channel currents contribute to neuronal hyperexcitability and subsequent AWS remain unknown. It is thought that the elevated Ca_V channel currents trigger increases in intracellular Ca^{2+} and that these increases in intracellular Ca^{2+} in turn activate several Ca^{2+}-dependent mechanisms, including Ca^{2+} release from intracellular Ca^{2+} pools, Ca^{2+}-activated K^+ channels and Ca^{2+}-activated chloride channels. Whether these mechanisms are altered at 3 h following alcohol withdrawal remains unknown.

The nature and phenotype of the IC neurons evaluated in this study were not identified. The IC contains both GABAergic (~25%) and non-GABAergic neurons (~75%; Ito & Oliver, 2012). We have previously reported that an elevated incidence of AWS is associated with a loss of GABA-mediated inhibition and elevated glutamatergic function in IC neurons (N'Gouemo et al., 1996; Evans et al., 2000; Faingold et al., 2000). Interestingly, these IC neurons also exhibited elevated Ca_V channel currents and reduced large-conductance Ca^{2+}-activated K^+ currents (N'Gouemo and Morad, 2003, 2013). It is likely that the downregulation of GABA receptors and large-conductance Ca^{2+}-activated K^+ channels, together with the upregulation of Ca_V channels and glutamate receptors, results in the generation of bursts of action potentials, leading to increased neuronal excitability during alcohol withdrawal.

The present study is the first to demonstrate that high-threshold Ca_V current density is enhanced in IC neurons before the onset of AWS and that inhibition of L- and to a lesser extent of P-type Ca_V channels within the IC suppresses these seizures. Because L-type Ca_V channels play an important role in the control of neuronal excitability, and inhibiting these channels markedly suppressed the occurrence of GTCS, these data provide a possible molecular mechanism for the pathogenesis of neuronal hyperexcitability that leads to AWS.

Acknowledgments

Role of funding source

This work was supported by the NIAAA Grant R01AA020073 (P.N). NIAAA has no further role in the study design; in the collection, analysis and interpretation of data; and in the decision to submit the paper for publication.

This work was supported by Public Health Service Grant R01AA020073 (P.N.) from the National Institutes of Health (NIH), and its contents are the responsibility of the author and do not necessary represent the official view of NIH.

References

Chakravarty DN, Faingold CL. Comparison of neuronal response patterns in the external and central nuclei of inferior colliculus during ethanol administration and ethanol withdrawal. Brain Res. 1998; 783:102–108. [PubMed: 9479057]

Eckardt MJ, Campbell GA, Marietta CA, Majchrowicz E, Wixon HN, Weight FF. Cerebral 2-deoxyglucose uptake in rats during ethanol withdrawal and post-withdrawal. Brain Res. 1986; 366:1–9. [PubMed: 3697671]

Ermolyuk YS, Alder FG, Surges R, Pavlov IY, Timofeeva Y, Kullmann DM, et al. Differential triggering of spontaneous glutamae release by P/Q-, N-, and R-type Ca2+ channels. Nat Neurosci. 2013; 16:1754–1763. [PubMed: 24185424]

Evans MS, Li Y, Faingold CL. Inferior colliculus intracellular response abnormalities in vitro associated with susceptibility to ethanol withdrawal seizures. Alcoholism: Clin Exp Res. 2000; 24:1180–1186.

Faingold CL. The Majchrowicz binge alcohol protocol: an intubation technique to study alcohol dependence in rats. Curr Protoc Neurosci. 2008 Jul.Chapter 9(Unit9.28)

Faingold CL, Riaz A. Ethanol withdrawal induces increased firing in the inferior colliculus neurons associated with audiogenic seizure susceptibility. Exp Neurol. 1995; 132:91–98. [PubMed: 7720830]

Faingold CL, N'Gouemo P, Riaz A. Ethanol and neurotransmitter interaction-from molecular to integration effects. Prog Neurobiol. 1998; 55:509–535. [PubMed: 9670216]

Faingold CL, Li Y, Evans MS. Decreased GABA and increase glutamate-mediated activity on inferior colliculus neurons in vitro are associated with susceptibility to ethanol withdrawal seizures. Brain Res. 2000; 868:287–295. [PubMed: 10854581]

Frye GD, McCown TJ, Breese GR. Characterization of susceptibility to audiogenic seizures in ethanol-dependent rats after microinjection of gamma-aminobutyric acid (GABA) agonists into the inferior colliculus, substantia nigra or medial septum. J Pharmacol Exp Ther. 1983; 227:663–670. [PubMed: 6317842]

Hamill OP, Marty A, Neher E, Sakmann B, Sigworth FJ. Improved patch-clamp techniques for high-resolution current recording from cells and cell-free membrane patches. Pflugers Arch-Eur J Physiol. 1981; 391:85–100. [PubMed: 6270629]

Heinemann U, Lux HD, Gutnick MJ. Extracellular free calcium and potassium during paroxysmal activity in the cerebral cortex of the cat. Exp Brain Res. 1977; 27:237–243. [PubMed: 880984]

Huang GJ, McArdle JJ. Chronic ingestion of ethanol increases the number of Ca^{2+} channels of hippocampal neurons of long-sleep but not short-sleep mice. Brain Res. 1993; 615:328–330. [PubMed: 8395960]

Ito T, Oliver DL. The basic circuit of the IC: tectothalamic neurons with different patterns of synaptic organization send different messages to the thalamus. Front Neural Circuits. 2012; 6:48, 1–9. [PubMed: 22855671]

Li Y, Evans MS, Faingold CL. Inferior colliculus neurons membrane and synaptic properties in genetically epilepsy-prone rats. Brain Res. 1994; 660:232–240. [PubMed: 7820692]

Little HJ, Dolin SJ, Halsey MJ. Calcium channel antagonists decrease the ethanol withdrawal syndrome. Life Sci. 1986; 39:2059–2065. [PubMed: 3784769]

Majchrowicz E. Induction of physical dependence on alcohol and the associated metabolic and behavioral changes in rats. Psychopharmacologia. 1975; 43:245–254. [PubMed: 1237914]

McCown TJ, Breese GR. Multiple withdrawals from chronic ethanol "kindles" inferior collicular seizure activity: evidence for kindling seizures associated with alcoholism. Alcohol: Clin Exp Res. 1990; 14:394–399. [PubMed: 2378423]

McCown TJ, Breese GR. A potential contribution to ethanol withdrawal kindling: reduced GABA function in inferior collicular cortex. Alcohol: Clin Exp Res. 1993; 17:1290–1294. [PubMed: 8116844]

Millan MH, Meldrum BS, Faingold CL. Induction of audiogenic seizure susceptibility by focal infusion of excitant amino acid or bicuculline into the inferior colliculus of normal rats. Exp Neurol. 1986; 91:634–639. [PubMed: 3512285]

N'Gouemo P, Morad M. Ethanol withdrawal seizure susceptibility is associated with upregulation of L- and P-type Ca^{2+} channels currents in rat inferior colliculus neurons. Neuropharmacology. 2003; 45:429–437. [PubMed: 12871660]

N'Gouemo P, Morad M. Alcohol withdrawal is associated with a downregulation of large-conductance Ca^{2+}-activated K^{+} channels in rat inferior colliculus neurons. Psychopharmacology. 2013; 231:2009–2018. [PubMed: 24241791]

N'Gouemo P, Caspary DM, Faingold CL. Decreased GABA effectiveness in the inferior colliculus neurons during ethanol withdrawal in rat susceptible to audiogenic seizures. Brain Research. 1996; 724:200–204. [PubMed: 8828569]

N'Gouemo, P.; Akinfiresoye, LR.; Allard, SA.; Lovinger, DM. Alcohol withdrawal-induced seizure susceptibility is associated with an upregulation of CaV1.3 channels in rat inferior colliculus neurons. Int J Neuropsychopharmacol. 2015. http://dx.doi.org/10.1093/ijnp/pyu123

Paxinos, G.; Watson, C. The rat brain in stereotaxic coordinates. Academic Press; San Diego: 1998.

Riaz A, Faingold CL. Seizures during ethanol withdrawal are blocked by focal microinjection of excitant amino acid antagonists in the inferior colliculus and pontine reticular formation. Alcohol: Clin Exp Res. 1994; 18:1456–1462. [PubMed: 7695044]

Thiagarajan TC, Lindskog M, Tsien RW. Adaptation to synaptic inactivity in the hippocampal neurons. Neuron. 2005; 47:725–737. [PubMed: 16129401]

Ueda Y, Tusru N. Simultaneous monitoring of the seizure related change in extracellular glutamate and gamma-aminobutyric acid concentration in bilateral hippocampi following development of amygdaloid kindling. Epilepsy Res. 1995; 20:213–219. [PubMed: 7796793]

Whittington MA, Little HJ. Change in voltage-operated calcium channel modifying ethanol withdrawal hyperexcitability in mouse hippocampal slices. Br J Pharmacol. 1993; 103:1313–1320. [PubMed: 1832063]

Whittington MA, Lambert JD, Little HJ. Increases in synaptic activation of calcium current as a mechanism for generation of alcohol withdrawal seizures. Alcohol Alcohol Suppl. 1993; 2:391–394. [PubMed: 7748328]

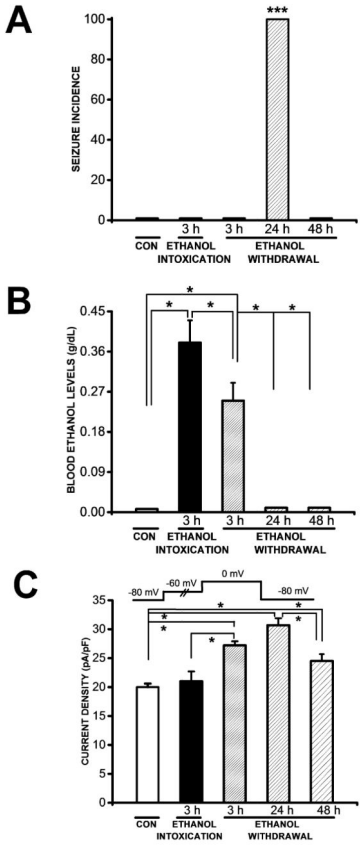

Figure 1.

Seizure incidence, blood ethanol levels and Ba^{2+} currents. **A**. At 24 h during ethanol withdrawal, all tested animals (n=10) exhibited wild running seizures (WRS) that evolved into bouncing generalized tonic-clonic seizures (clonus). No seizure susceptibility was observed 3 h (n=8) or 48 h (n=8) during ethanol withdrawal or in the control group (n=8) or 3 h after ethanol intoxication. The seizure incidence was significantly ($P<0.001$; χ^2) elevated 24 h compared with 3 h and 48 h during ethanol withdrawal, 3 h after ethanol intoxication and the control group. **B.** Blood ethanol concentrations (BECs) were also significantly elevated 3 h during ethanol intoxication (n=6) compared with the control group (n=6, $P<0.05$, Bonferroni's test) and the group tested 3 h during ethanol withdrawal (n=6, $P<0.05$, Bonferroni's test). During ethanol withdrawal, BECs were significantly elevated 3 h (n=6, $P<0.05$, Bonferroni's test) but negligible 24 h (n=6) and 48 h (n=6) during ethanol withdrawal compared with the control group (n=6). BECs measured 3 h during ethanol withdrawal were significantly (n=6, $P<0.05$, Bonferroni's test) elevated compared with 24 h or 48 h during ethanol withdrawal. **C.** The mean peak Ba^{2+} current density in IC neurons was significantly higher 3 h (n=14, $P<0.05$, Bonferroni's test), 24 h (n=18, $t=5.9$, $P<0.05$, Bonferroni's test) and 4h (n=16, $t=3$, $P<0.05$, Bonferroni's test) during ethanol withdrawal than in the control group (n=18). The current density was also significantly higher 24 h (n=18, $P<0.05$, Bonferroni's test) than 48 h (n=16) following ethanol withdrawal. The mean peak Ba^{2+} current density 3 h (n=14, $P<0.05$, Bonferroni's test) following ethanol withdrawal was significantly enhanced in IC neurons compared with 3 h (n=10) after

ethanol intoxication. The current density was not altered in IC neurons after ethanol intoxication compared with the control group. Ba^{2+} currents were activated as shown in the inset. Each bar graph represents the mean ± S.E.M or percentage (%). *P<0.05, ***P<0.001.

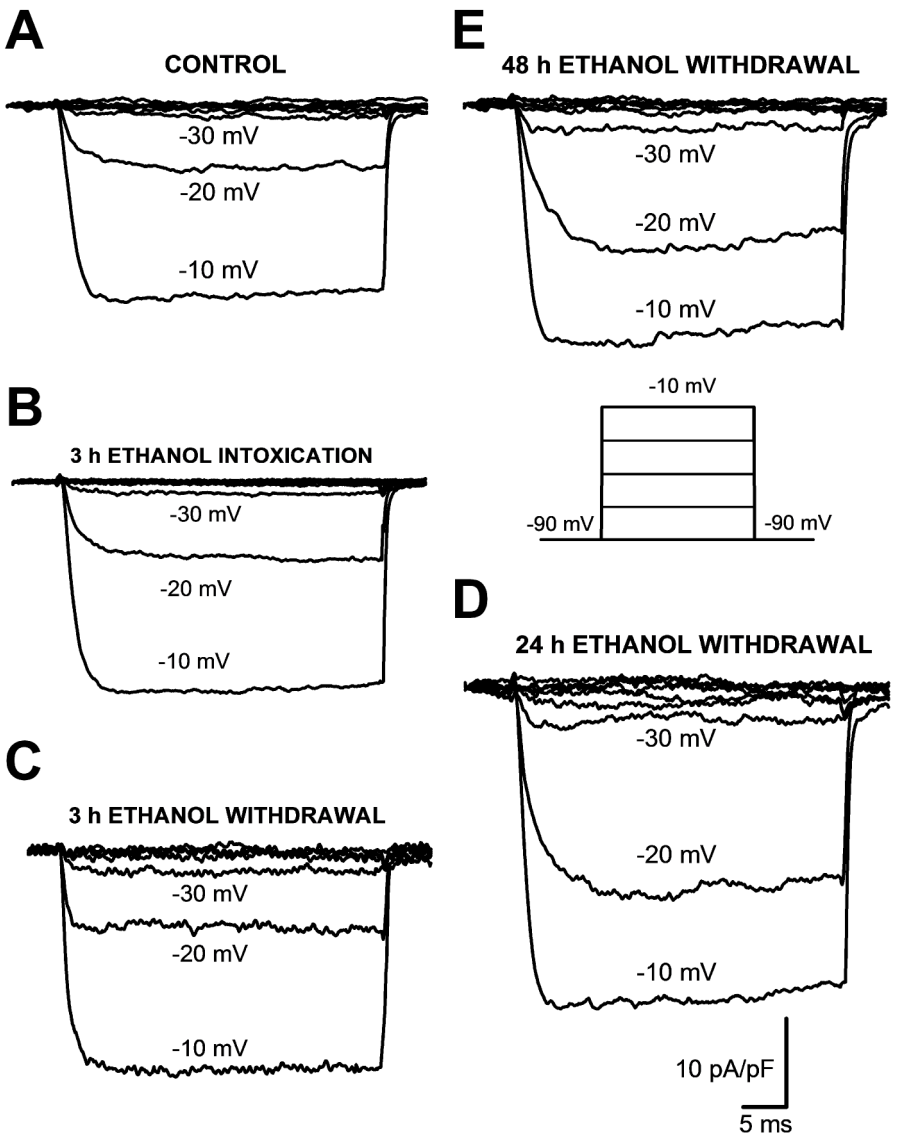

Figure 2.

Representative traces of whole-cell Ba^{2+} currents activated by different voltages in IC neurons obtained from the control group (panel **A**), 3 h after ethanol intoxication (panel **B**) or 3 h (panel **C**), 24 h (panel **D**) or 48 h (panel **E**) during ethanol withdrawal. Of particular interest, the peak current density at −20 mV was enhanced 0.1-fold, 2.3-fold and 1.3-fold 3 h (−8 pA/pF), 24 h (−23 pA/pF) and 48 h (−16 pA/pF) during ethanol withdrawal, respectively, compared with the control group (−7 pA/pF). The peak current density at −20 mV was not altered 3 h after ethanol intoxication (−8 pA/pF) compared with the control group (−7 pA/pF). Whole-cell Ba^{2+} currents were activated as shown in the inset (panel **E**).

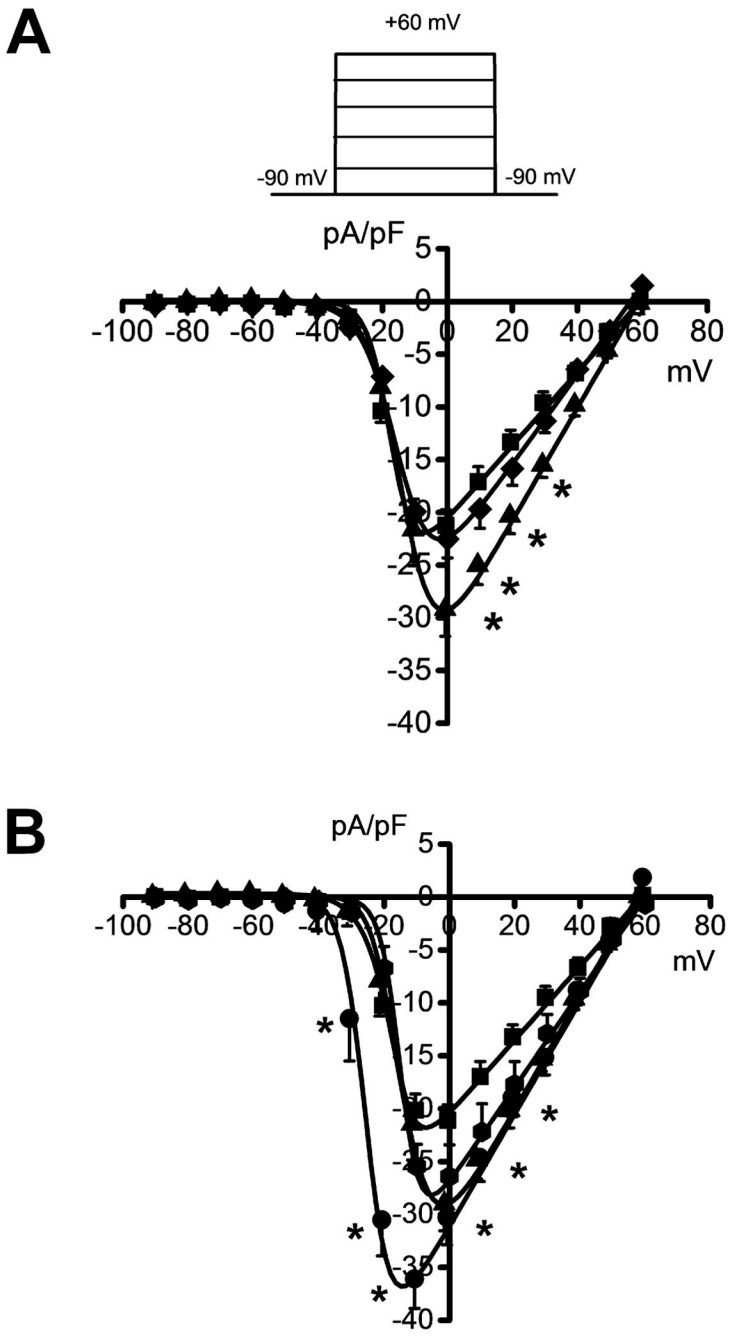

Figure 3.

Altered voltage-dependence of Ba^{2+} currents during ethanol withdrawal. The average peak current density-voltage curves were fitted using a modified Boltzmann function (see Materials and Methods). For comparison, the voltage dependence of the currents in IC neurons from three (panel A) and four (panel B) conditions are plotted. Ba^{2+} currents were activated as shown in the inset (panel A). **A**. The current density was significantly increased ($P<0.05$, Bonferroni's test) in IC neurons obtained 3 h (filled triangles, n=10) during ethanol withdrawal at voltages positive to 0 mV compared with the control group (filled squares,

n=14). The current density measured at the 0 mV voltage step 3 h following ethanol withdrawal (filled triangles, n=10) was significantly (P<0.05, Bonferroni's test) elevated compared with 3 h during ethanol intoxication (filled diamonds, n=7). **B.** The current density was increased in IC neurons obtained 24 h (filled circles, n=10) during ethanol withdrawal at voltages between −40 mV and +40 mV compared with the control group (filled squares, n=14). The current density at 24 h following ethanol withdrawal (n=10) also was significantly (P<0.05, Bonferroni's test) elevated at voltages negative to 0 mV compared with 3 h (filled triangles, n=10) and 48 h following ethanol withdrawal. Each point represents the mean ± S.E.M. **P*<0.05.

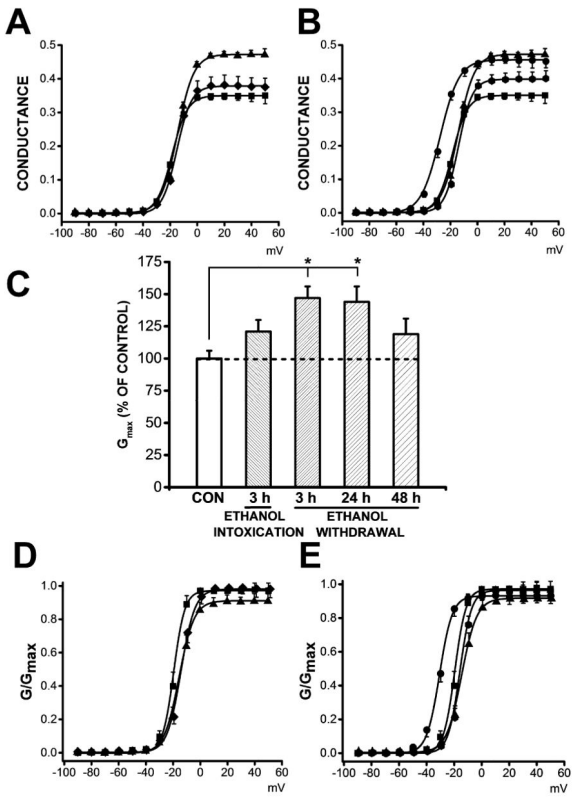

Figure 4.

Altered Ba^{2+} conductance and channel activation during ethanol withdrawal. **A.** Plots of normalized conductance as a function of voltage in IC neurons from the control group, 3 h during ethanol intoxication and 3h during ethanol withdrawal. Quantification revealed that at positive voltages, the conductance was increased by 34% 3 h (n=10, filled triangles) during ethanol withdrawal compared to the control group (n=14, filled squares). Only a 9% increase was observed 3 h after ethanol intoxication (n=7, filled diamonds) compared with the control group (n=14, filled squares). **B.** Plots of normalized conductance as a function of voltage in IC neurons from the control group, 3, 24 and 48 h during ethanol withdrawal. Plots of normalized conductance as a function of voltage revealed that conductance was enhanced in IC neurons at positive by 34%, 31%, and 14% at 3 h (n=10, filled triangles), 24 h (n=11, filled circles), and 48 h (filled octagons) after the withdrawal of ethanol, respectively, relative to the control group (n=14, filled squares). **C.** The mean maximal conductance, G_{max}, calculated using a modified Boltzmann function (see Materials and Methods), was significantly enhanced in IC neurons 3 h n=10, $P<0.05$, Bonferroni's test) and 24 h (n=11, $P<0.05$, Bonferroni's test) during ethanol withdrawal compared with the control group (n=14). G_{max} values were non-significantly increased 3 h during ethanol intoxication (n=7) compared with the control group (n=14, filled squares). Similarly, G_{max} values were non-significantly increased 3 h after ethanol intoxication compared with 3 h during ethanol intoxication (n=10). **D**. G/G_{max} curves are plotted in three conditions: control group (n=14, filled squares), 3 h during ethanol intoxication (n=7, filled diamonds) and 3 h during ethanol withdrawal (n=10, filled triangles). G/G_{max} curves fitted with a modified Boltzmann function (see Materials and Methods) were not altered during ethanol

intoxication or withdrawal (3 h group) compared to the control group. **F**. G/G_{max} curves are plotted in four conditions: control group, 3, 24 and 48 h during ethanol withdrawal. G/G_{max} curves fitted with a modified Boltzmann function indicate a shift toward negative values 24 h during ethanol withdrawal (n=11, filled circles) compared with 3 h (n=10, filled triangles) and 48 h (n=10, filled octagons) during ethanol withdrawal, as well as with the control group (n=14, filled squares). Each point represents the mean± S.E.M.

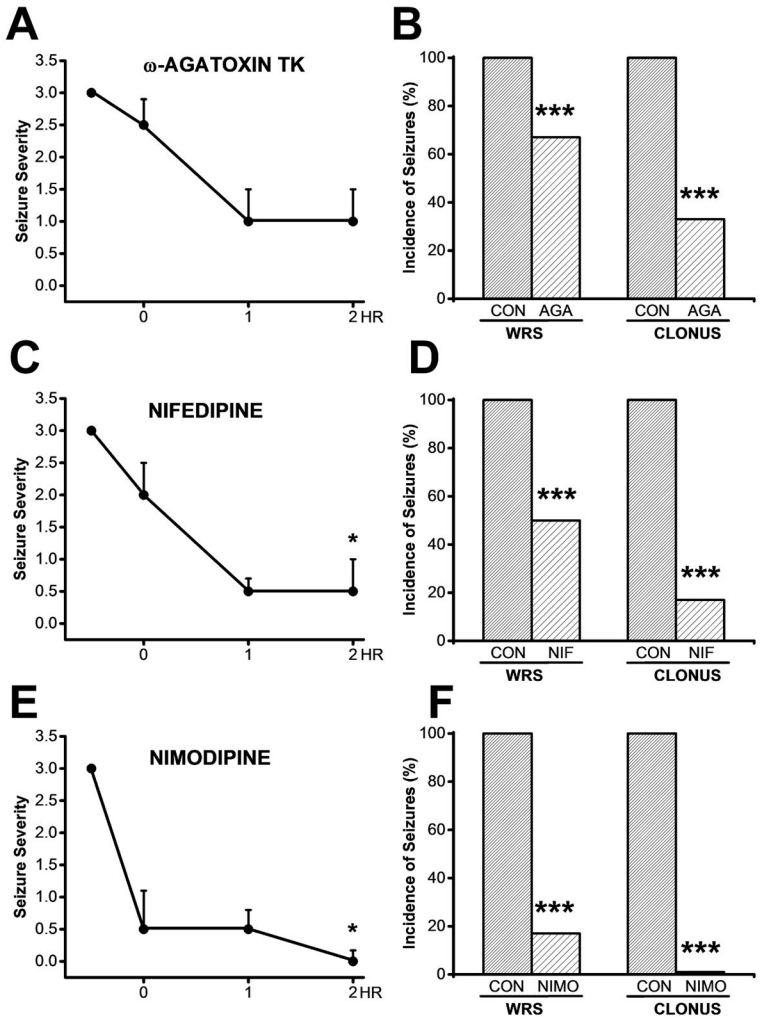

Figure 5.

Effects of bilateral microinjection of Ca_V1 channel blockers into the IC on the susceptibility to acoustically evoked seizures following ethanol withdrawal. **A**. The time course of the effects of bilateral microinjections of ω-agatoxin TK (30 nM/side) showed no significant reduction in the median score of seizure severity from 3 to 2.5, 1 and 1at 0.5, 1 and 2 h post infusion, respectively, compared to pre-infusion (n=6, P<0.2, Kruskal Wallis test). **B.** Microinjection of ω-agatoxin TK significantly reduced the incidence of WRS and clonus by 33% (P<0.001, χ^2) and 67% (P<0.001, χ^2), respectively, by 2 h post-infusion during the ethanol withdrawal period compared with pre-infusion. **C**. The time course of the effects of bilateral microinjections of nifedipine (10 μM/side) showed a significant reduction of the median score of seizure severity from 3 to 2, 0.5 and 0.5 at 0.5, 1 and 2 h post-infusion compared to pre-infusion (n=6, P<0.05, Kruskal-Wallis test). **D.** Bilateral microinjections of nifedipine significantly reduced the occurrence of WRS and clonus by 50% (P<0.001, χ^2) and 83% (P<0.001,, χ^2), respectively, by 2 h post-infusion during the ethanol withdrawal. **E.** The time course of the effects of bilateral microinjections of nimodipine (1 μM/side) showed a suppression of the median score of seizure severity from 3 to 0.5, 0.5 and 0 at 0.5, 1, and 2

h post-infusion during ethanol withdrawal (n=6, P<0.05, Kruskal Wallis test). **F.** Microinjection of nimodipine significantly reduced the occurrence of WRS (n=6, P<0.001, χ^2) and completely suppressed the occurrence of clonus (n=6, P<0.001, χ^2) at 2 h post-infusion during the ethanol withdrawal period. Each point and bar graph represents the mean ± S.E.M and percentage (%), respectively. *P<0.05, ****P<0.001.